ELSEVIER

Journal of Power Sources 66 (1997) 61–69

JOURNAL OF POWER SOURCES

Mathematical analysis of potential losses in a thick porous metal-hydride electrode during a discontinuous discharge

J. Heikonen *

Institute of Mathematics, Helsinki University of Technology, Otakaari 1M, 02150 Espoo, Finland

Received 6 September 1996; accepted 26 September 1996

Abstract

We consider a thick porous metal-hydride electrode in a temporarily interrupted discharge. During a break the hydrogen and electrolyte concentrations tend to level steady states, which leads to a recovery phenomenon seen in the decrease in potential loss in the electrode when the discharge is restarted. A mathematical model is used in studying the electrochemical system. The potential loss is expressed as a sum of potential losses due to various sources, and spatial averaging is used in analyzing the individual losses as well as the reaction conditions. Furthermore, a simple model is developed for describing the behavior of the hydrogen concentration during a break.

Keywords: Metal-hydride electrodes; Mathematical analysis; Potential losses

1. Introduction

We are working on the development of a battery with a metal-hydride (MH) electrode for electric-vehicle use. In this kind of application the battery is discharged with a strongly varying current. Furthermore, the discharge is frequently completely interrupted. In this paper we investigate the performance of a thick MH electrode over a discharge break using a mathematical model.

Mathematical models for MH electrodes are presented in Refs. [1–3], for example. A complete cell with a thin MH electrode is modeled in Ref. [4]. Recovery or relaxation phenomena for cells with different electrodes have been considered in Refs. [5,6].

In this paper, we use the model developed in Ref. [3], but reconsider the potential losses in more detail, and keeping in mind the interrupted discharge. As before, we use spatial averaging to analyze the potential losses due to various mechanisms. Moreover, the averaging method is applied in studying the reaction conditions, such as the electrolyte and hydrogen concentrations and the reaction rate density.

Our mathematical model is simple so that analytic methods can be applied more easily in investigating the simulations results. On the other hand, with a simple model one looses some accuracy; this model should only be used to study and interpret phenomena and their relationship in a thick MH electrode instead of trying to produce precise predictions for specific quantities.

2. Mathematical model

A brief description of the mathematical model is given; more details can be found in Ref. [3].

2.1. Porous MH electrode and the cell

The porous MH electrode is manufactured by bonding MH particles together with polytetrafluoroethylene (PTFE) and carbon. In the cell the MH electrode is immersed in KOH electrolyte.

The void volume fraction, i.e. the porosity of the electrode is denoted by ϵ. Let ν be the volume fraction of the MH alloy in the electrode. Due to the passive bonding material $\epsilon+\nu<1$. The porosity and tortuosity of the electrode are taken into account by multiplying the ionic diffusion coefficients $D^{\pm}_{\text{free}}$ and conductivities $\sigma^{\pm}_{\text{free}}$ by $\epsilon^{1.5}$. The subscript 'free' refers to solution outside any porous structure. We define the effective ionic diffusion coefficients and conductivities by

$$D^{\pm}=\epsilon^{1.5}D^{\pm}_{\text{free}},\ \sigma^{\pm}=\epsilon^{1.5}\sigma^{\pm}_{\text{free}} \tag{1}$$

In this article, we concentrate on the MH electrode. Accordingly, the counter electrode is viewed only as a source

* Corresponding author.

PII S0378-7753(96)02481-0

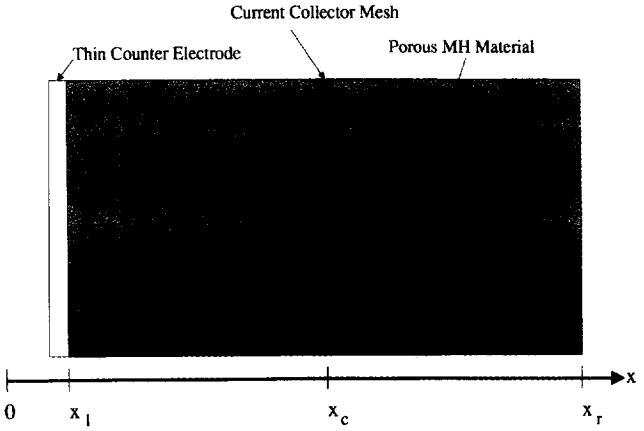

Fig. 1. Schematic diagram of the electrode system. The section of the cell tube with the electrodes is shown straightened here. The circular tube is formed when the point $x=L$ (far right, not shown) is connected with the point $x=0$.

of ions and modeled as very thin. In laboratory experiments a nickel mesh, for example, can be the thin counter electrode. Its location is denoted by x_l. The locations of the left and right ends of the MH electrode are denoted by x_l and x_r, respectively. The thin current collector is placed at the mid point of the MH electrode at $x_c=(x_l+x_r)/2$, see Fig. 1.

We use the same cell geometry as in Refs. [3,7], that is, we consider a circular cell. Note that this is only a mathematical model and not a description of a real practical cell. As we make L, the total length of the cell tube, large compared with x_r-x_l, the thickness of the MH electrode, the situation corresponds to two electrodes in a large reservoir of electrolyte. This is a typical experimental setup in testing MH electrodes. To avoid discontinuities in the diffusion coefficients and the conductivities we assume that outside the electrodes the tube is filled with a passive porous material having the same porosity as the MH electrode.

Finally, the discharge flux density is denoted by J.

2.2. Reaction kinetics

The operation of an MH electrode is based on the reaction

$$MH_{ads}+OH^- \rightleftharpoons e^- + H_2O + M \tag{2}$$

We use a very simple Butler–Volmer-type expression [8] to describe the reaction kinetics of Eq. (2). Let c and h_s be the electrolyte concentration and the concentration of hydrogen on the surface of a MH particle, respectively. The concentration of water is assumed to be constant and denoted by c_{H_2O}. The reaction rate density, r (mol/(m^3 s)), can then be modeled by

$$r(t,x)=\frac{\nu\rho}{F}\left[k_a\exp\left\{\frac{0.5FV(t,x)}{RT}\right\}c(t,x)h_s(t,x) - k_c\exp\left\{-\frac{0.5FV(t,x)}{RT}\right\}c_{H_2O}\right] \tag{3}$$

where

$$V(t,x)=\varphi(t,x)-\phi(t,x) \tag{4}$$

is the difference between the potential in the solid and the potential in the electrolyte, denoted by φ and ϕ, respectively, measured with a Hg/HgO reference electrode. Furthermore, k_a and k_c are the reaction rate constants and T is temperature, which is assumed to be constant. Since we measure exchange current density in A/g we have included the factor $\nu\rho/F$, where ρ is the mass density of the MH alloy, in Eq. (3).

2.3. Ion transport in the electrolyte

The ions are driven by diffusion and migration in the electrolyte. The motion of the ions is modeled with a dilute solution theory from Ref. [8] using constant ionic diffusion coefficients and ionic conductivities. The electrolyte concentration c and potential ϕ satisfy the equations

$$\epsilon c_t(t,x)=-\frac{\partial}{\partial x}\left(-D^-c_x(t,x)+\frac{\sigma^-}{F}\phi_x(t,x)\right)+E(t,x) \tag{5}$$

$$\epsilon c_t(t,x)=-\frac{\partial}{\partial x}\left(-D^+c_x(t,x)-\frac{\sigma^+}{F}\phi_x(t,x)\right) \tag{6}$$

which describe the motion of the OH^- and K^+ ions, respectively.

The inhomogeneous term, E, in Eq. (5) represents the effect of the electrode reactions. OH^- ions are produced on the thin counter electrode with the rate corresponding to the discharge flux density, J, and consumed in the MH electrode with the rate, r, given by Eq. (3). Accordingly

$$E(t,x)=J(t)\delta_{x_l}(x)-r(t,x) \tag{7}$$

where a Dirac delta function δ_{x_l} is used in describing the thin counter electrode. The K^+ ions do not take part in the reactions and, hence, there is no corresponding term in Eq. (6).

Due to the conservation of charge, the condition

$$\int_{x_l}^{x} r(t,\xi)\,d\xi = J(t) \tag{8}$$

must hold for all $t>0$.

Mathematically the circular tube is described by periodic boundary conditions. We require that the electrolyte concentration and potential and the electric field at $x=L$ coincide with the their respective values at $x=0$. More precisely

$$c(t,0)=c(t,L) \tag{9}$$

$$\phi(t,0)=\phi(t,L) \tag{10}$$

$$\phi_x(t,0)=\phi_x(t,L) \tag{11}$$

We emphasize that these quantities are not periodic over the MH electrode but over the whole cell tube.

In the beginning of the discharge the electrolyte concentration is constant everywhere. Therefore, we have the initial condition

$$c(0,x)=c_0. \tag{12}$$

2.4. Hydrogen diffusion in MH material

The hydrogen diffusion is modeled in a simplified geometry. By scaling the diffusion coefficient we make sure that the time scale of the hydrogen diffusion remains correct.

Let Z, the maximal diffusion distance in the model, be

$$Z = \nu/\gamma \tag{13}$$

where γ is the active surface area density (m^2/m^3) of the MH alloy. Next, we define the scaled diffusion coefficient, d, by

$$d = Z^2/t_{diff} = \nu^2/(\gamma^2 t_{diff}) \tag{14}$$

where t_{diff} is the characteristic time of the hydrogen diffusion. Finally, the characteristic time of the hydrogen diffusion is defined by

$$t_{diff} = r_{MH}^2/D^H \tag{15}$$

where r_{MH} is a typical diffusion distance in real MH particles and D^H is the diffusion coefficient.

Designate the concentration of hydrogen in the MH material by h. We model the hydrogen diffusion with the basic diffusion equation

$$h_t(t,z,x) = dh_{zz}(t,z,x) \tag{16}$$

where $t > 0$, $0 < z < Z$ and $x_l < x \le x_r$. In this section x is only a parameter. The boundary condition

$$\gamma dh_z(t,Z,x) = -r(t,x) \tag{17}$$

models the hydrogen flow through surfaces of particles due to the reaction (2). The other boundary condition

$$dh_z(t,0,x) = 0 \tag{18}$$

corresponds to a symmetry condition in the middle of a real particle. We assume that the initial hydrogen concentration is constant throughout the MH electrode

$$h(0,z,x) = h_0 \tag{19}$$

Finally, the surface concentration of hydrogen, h_s, is defined by

$$h_s(t,x) = h(t,Z,x) \tag{20}$$

2.5. Electric current in the electrode material

Using Ohm's law we obtain an equation for the potential φ in the electrode material

$$\kappa\varphi_{xx}(t,x) = F(r(t,x) - J(t)\delta_{x_c}(x)) \tag{21}$$

where κ is the effective electric conductivity of the electrode material. The thin current collector at $x_c = (x_l + x_r)/2$ is modeled with a Dirac delta function δ_{x_c}. In Eq. (21) $x_l < x < x_r$ and t is only a parameter.

The boundary conditions

$$\varphi_x(t,x_l) = 0 \tag{22}$$

and

$$\varphi_x(t,x_r) = 0 \tag{23}$$

state that the ends of the electrode are insulated.

3. Potential losses and reaction conditions

We define the electrode potential Φ to be the potential difference between the current collector and the electrolyte between the counter and MH electrodes

$$\Phi(t) = \varphi(t,x_c) - \phi(t,x_l) \tag{24}$$

The electrode potential is measured with a Hg/HgO reference electrode. The local momentary equilibrium potential V_0 and the steady-state open-circuit equilibrium potential $V_{0,\infty}$ are obtained from Eq. (3) by setting $r = 0$ and using appropriate electrolyte and hydrogen concentrations

$$V_0(t,x) = \frac{RT}{F}\ln\left\{\frac{k_c}{k_a}\frac{c_{H_2O}}{c(t,x)h_s(t,x)}\right\} \tag{25}$$

and

$$V_{0,\infty}(t) = \frac{RT}{F}\ln\left\{\frac{k_c}{k_a}\frac{c_{H_2O}}{c_0(1 - t/t_{max})h_0}\right\} \tag{26}$$

where

$$t_{max} = \frac{\nu(x_r - x_l)h_0}{J} \tag{27}$$

is the maximal theoretical discharge time when the electrode is discharged with the constant flux density, J. If the current is switched off at $t = t_c$ then

$$\lim_{t\to\infty} V_0(t,x) = V_{0,\infty}(t_c) \tag{28}$$

We may define the total potential loss in the electrode

$$V_{loss}(t) = \Phi(t) - V_{0,\infty}(t) \tag{29}$$

As in Ref. [3] we divide the total potential loss into four components: (i) the potential loss in the electrolyte, η_l; (ii) the reaction overpotential, η; (iii) the potential loss in the solid phase η_s, and (iv) the loss due to concentration polarization (the deviation of the local momentary equilibrium potential from the steady-state open-circuit equilibrium potential), η_p. Both electrolyte and hydrogen concentration polarization contribute to η_p. To be more precise

$$\eta_l(t,x) = \phi(t,x) - \phi(t,x_l) \tag{30}$$

$$\eta(t,x) = V(t,x) - V_0(t,x) \tag{31}$$

$$\eta_s(t,x) = \varphi(t,x_c) - \varphi(t,x) \tag{32}$$

and

$$\eta_p(t,x) = V_0(t,x) - V_{0,\infty}(t) \tag{33}$$

To describe the total significance of a individual loss component at a given time with a single number we first compute

the total power loss per projected area (W/m^2) due to the loss source in question. For example, consider the potential loss in the electrolyte. Since the total length of the cell tube is large compared with the thickness of the MH electrode, it is reasonable to assume here that the current outside the MH electrode is negligible. The current density for $x_l \le x \le x_r$ is

$$F\left(J-\int_{x_l}^{x} r(t,\eta)\,d\eta\right) \tag{34}$$

so that the total power loss in the MH electrode due to the resistance of the electrolyte is

$$\begin{aligned}
&\int_{x_l}^{x_r} F\left(J-\int_{x_l}^{\xi} r(t,\eta)\,d\eta\right)\phi_x(t,\xi)\,d\xi \\
&= F\left(J-\int_{x_l}^{\xi} r(t,\eta)\,d\eta\right)\phi(t,\xi)\,|_{x=x_l}^{x=x_r} + \int_{x_l}^{x_r} Fr(t,\xi)\,\phi(t,\xi)\,d\xi \\
&= \int_{x_l}^{x_r} Fr(t,\xi)\,\phi(t,\xi)\,d\xi - FJ\phi(t,x_l) \\
&= \int_{x_l}^{x_r} Fr(t,\xi)\,(\phi(t,\xi)-\phi(t,x_l))\,d\xi \\
&= \int_{x_l}^{x_r} Fr(t,\xi)\,\eta_l(t,\xi)\,d\xi
\end{aligned} \tag{35}$$

Now the corresponding average potential loss in the electrolyte $\overline{\eta_l}$ is obtained by dividing the power loss density by the current density

$$\overline{\eta_l}(t) = \frac{\int_{x_l}^{x_r} Fr(t,\xi)\,\eta_l(t,\xi)\,d\xi}{\int_{x_l}^{x_r} Fr(t,\xi)\,d\xi} = \frac{\int_{x_l}^{x_r} r(t,\xi)\,\eta_l(t,\xi)\,d\xi}{J} \tag{36}$$

The remaining three average potential losses $\overline{\eta}$, $\overline{\eta_s}$, and $\overline{\eta_p}$ are computed similarly. We use the above-defined average quantities to explain the changes in the total potential loss in the MH electrode over a break in discharge.

We also compute the corresponding weighted averages of the electrolyte concentration and the surface concentration of hydrogen, denoted by $\overline{c}$ and $\overline{h_s}$:

$$\overline{c}(t) = \frac{\int_{x_l}^{x_r} r(t,\xi)\,c(t,\xi)\,d\xi}{J} \tag{37}$$

and

$$\overline{h_s}(t) = \frac{\int_{x_l}^{x_r} r(t,\xi)\,h_s(t,\xi)\,d\xi}{J} \tag{38}$$

Although there are no direct physical interpretations in these cases, these averaged quantities give us a clue to the time evolution of 'effective' reaction conditions. Furthermore, we define the average reaction rate density, $\overline{r}$, by

$$\overline{r}(t) = \frac{\int_{x_l}^{x_r} [r(t,\xi)]^2\,d\xi}{J} \tag{39}$$

This quantity reflects the localization of the reaction. The larger the value of $\overline{r}$ the more localized the reaction is. It is easy to show that $\overline{r}(t) \ge J/(x_r - x_l)$ for all t, where the lower limit corresponds to the situation in which the reaction rate density is constant throughout the MH electrode, and the reaction is fully spread out.

In addition to the fact that these averaged quantities describing the reaction conditions are interesting as such they can be used to study the averaged potential losses further. We apply the average electrolyte and hydrogen concentrations and the average reaction rate density in analyzing the average reaction overpotential and concentration of polarization loss. First we define the reference values for the reaction rate density, the surface concentration of hydrogen and the electrolyte concentration.

Let the reference reaction rate density, r_0, be

$$r_0 = \frac{J}{x_r - x_l} \tag{40}$$

That is, r_0 corresponds to the situation where the reaction rate density is constant throughout the MH electrode. Let $h_\infty(t)$ be the concentration that results if the total amount of hydrogen in the electrode at time t is evenly spread out. In other words

$$h_\infty(t) = (1 - t/t_{max})\,h_0 \tag{41}$$

The reference value for the electrolyte concentration is chosen to be c_0. In the following the electrolyte concentration, the surface concentration of hydrogen and the reaction rate density are considered relative to their reference values c_0, h_∞ and r_0, respectively.

We start with the reaction overpotential. Assume that the cathodic current is negligible during the discharge, we then easily obtain from Eq. (3)

$$V(t,x) \approx \frac{RT}{0.5F} \ln\left\{\frac{F^2}{\nu\rho k_a}\,\frac{r(t,x)}{c(t,x)\,h_s(t,x)}\right\} \tag{42}$$

Combining Eq. (42) with Eq. (25) yields after some manipulations an approximation for the reaction overpotential

$$\eta(t,x) \approx \frac{RT}{F} \ln\left\{\frac{F^2}{\nu^2\rho^2 k_a k_c c_{H_2O}}\,\frac{(r(t,x))^2}{c(t,x)\,h_s(t,x)}\right\} \tag{43}$$

By linearizing the previous expression with respect to the triple $(r_0, c_0, h_\infty(t))$ and substituting the result into the definition of the average loss we get

$$\overline{\eta}(t) \approx \frac{RT}{F}\left[\ln\left\{\frac{F^2}{\nu^2\rho^2 k_a k_c c_{H_2O}}\frac{r_0^2}{c_0 h_\infty(t)}\right\} + 2\left(\frac{\overline{r}(t)}{r_0}-1\right)-\left(\frac{\overline{c}(t)}{c_0}-1\right)-\left(\frac{\overline{h}_s(t)}{h_\infty(t)}-1\right)\right] \quad (44)$$

where we have ignored the residual term.

Similarly, the concentration polarization loss can be linearized

$$\overline{\eta}_p(t) \approx \frac{RT}{F}\left[\left(1-\frac{\overline{c}(t)}{c_0}\right)+\left(1-\frac{\overline{h}_s(t)}{h_\infty(t)}\right)\right] \quad (45)$$

Now we can use the averaged concentrations and the reaction rate density in Eqs. (44) and (45) in explaining the behavior of the reaction overpotential and the concentration polarization loss.

By using the averaging technique and removing the spatial dimension we, in a way, approximate the thick MH electrode with an infinitely thin one in which the averaged concentrations and the reaction rate density are the prevailing reaction conditions.

We emphasize that the approximative formulas derived above are presented only to help us to interpret the simulation results.

4. Simulation

Here we consider a case where the discharge is temporarily interrupted. The simulations predict a recovery phenomenon in the potential loss.

4.1. Parameters

The values of the parameters are given in Table 1. The concentration of water and the ionic diffusion coefficients and conductivities are determined for 6 mol/l KOH electrolyte. The reaction rate constants are computed assuming a fully charged electrode and the initial electrolyte concentration together with a measured equilibrium potential value of −0.927 V versus Hg/HgO and a measured exchange current density of 210 mA/g from Ref. [11].

The initial concentration of hydrogen is 1 wt.% in the MH alloy $LMNi_{3.6}Co_{0.7}Al_{0.4}Mn_{0.3}$ (Treibacher, Austria). The porosity and the MH material volume fraction as well as the thickness of the electrode are known from the preparation of prototype electrodes. The surface area density and the typical diffusion distance correspond to a precycled electrode.

The total length of the cell tube, L, is chosen large compared with $x_r - x_l$, the thickness of the MH electrode, so that the current outside the electrodes is negligible.

The electrode is discharged with a discharge flux density of 0.01 mol/m² s (100 mA/cm²) corresponding to $C/3.3$ rate. The reference reaction rate density is then 2.5 mol/(m³ s).

Table 1
General parameters

Parameter	Value	References
D^H	10^{-12} m²/s	[1]
D_{free}	3.33×10^{-9} m²/s	[9]
Λ_{free}	1.07×10^{-2} S m²/mol	[9]
t^+	0.22	[10]
D^+_{free}	2.13×10^{-9} m²/s	derived
D^-_{free}	7.57×10^{-9} m²/s	derived
σ^+_{free}	14.12 S/m	derived
σ^-_{free}	50.08 S/m	derived
k_a	4.4×10^{-4} m⁶/(kg mol s)	derived
k_c	5.7×10^{-16} m³/(kg s)	derived
κ	150 S/m	measured
c_0	6000 mol/m³	
c_{H_2O}	40000 mol/m³	
h_0	77400 mol/m³	
J	0.01 mol/(m² s)	
L	0.1 m	
x_l	0.001 m	
x_r	0.005 m	
γ	8×10^4 m²/m³	
ν	0.4	
ϵ	0.5	
ρ	7.74×10^3 kg/m³	
r_0	2.5 mol/(m³ s)	$J/(x_r-x_l)$
r_{MH}	15×10^{-6} m	
T	293 K	

4.2. Results

In this simulation the discharge is interrupted at 6000 s (the corresponding state-of-discharge is about 50%) and continued after a break of 7200 s.

Fig. 2 depicts V_{loss}, the total potential loss in the electrode. It can be seen that the potential loss immediately after the break is smaller than immediately before it. The difference is about 10 mV.

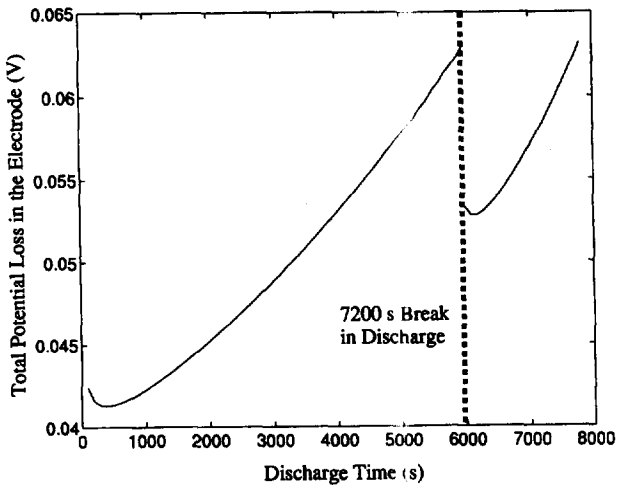

Fig. 2. Total potential loss in the MH electrode, V_{loss}. The curves before and after the break are separated with a dashed line

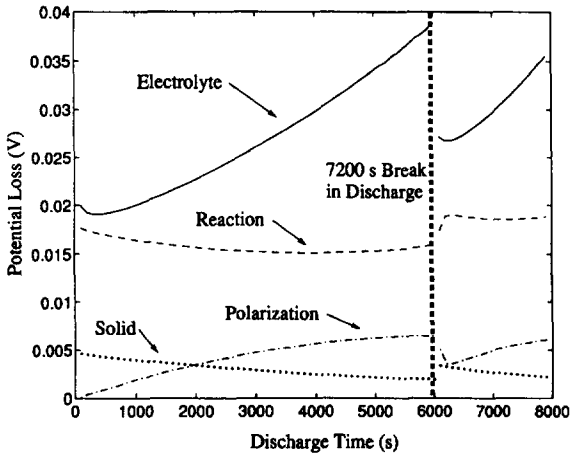

Fig. 3. Averaged potential losses $\overline{\eta_h}, \overline{\eta_s}, \overline{\eta_p}$, and $\overline{\eta}$. The curves before and after the break are separated with a dashed line.

In this case, the recovery is easily explained with Fig. 3 showing the averaged potential losses. The most important contribution to the decreased loss is the potential loss in the electrolyte, which decreases about 10 mV. The changes in reaction overpotential and concentration polarization loss cancel each other and the increase in potential loss in the solid is negligible.

We take now a closer look in the individual loss components. During the break the hydrogen concentration converges towards a level value, see Fig. 4. At the same time the electrolyte concentration also levels out as shown in Fig. 5. Thus the situation after the break resembles the start-of-discharge and the reaction zone starts again from the counter electrode, Fig. 6.

The decrease in potential loss in the electrolyte is caused by the reaction zone moving back to the counter electrode and the resulting shortening of the path of ions in the electrolyte. The potential loss in the solid increases since the distance between the reaction zone and the current collector gets longer.

We use the linear approximations (44) and (45) and the relative average electrolyte concentration $\bar{c}/c_0$, hydrogen concentration $\bar{h}_s/h_\infty$ and the relative average reaction rate

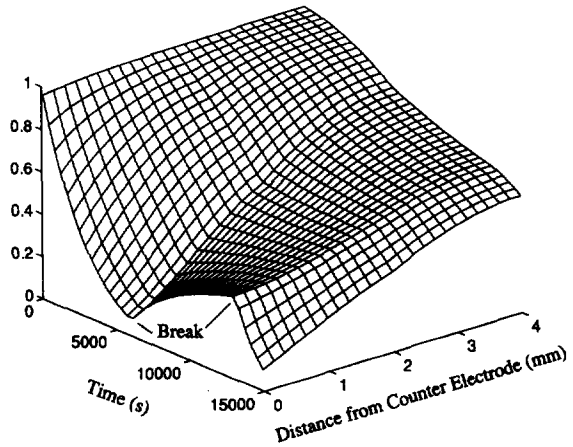

Fig. 4. Relative surface concentration of hydrogen, h_s/h_0. During the break the concentration tends to a level value of about 0.5.

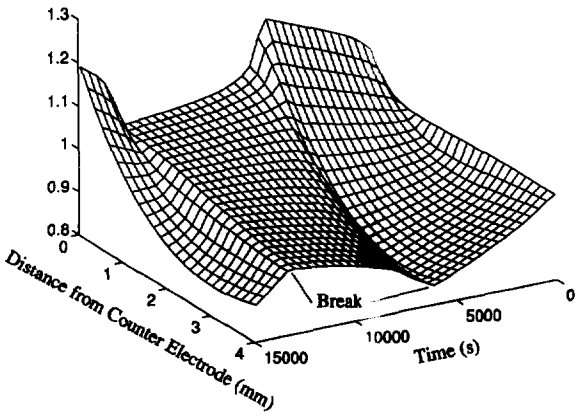

Fig. 5. Relative electrolyte concentration, c/c_0. During the break the concentration tends to the level initial value c_0.

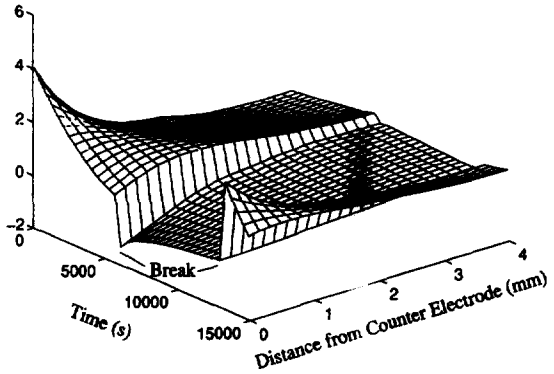

Fig. 6. Relative reaction rate density, r/r_0. The negative values during the break indicate charging related to the leveling of hydrogen.

density $\bar{r}/r_0$ shown in Fig. 7 to analyze the changes in reaction overpotential and concentration polarization loss. Generally, the reaction rate density varies the most while the changes in electrolyte and hydrogen concentrations are considerably smaller.

In the beginning of the discharge the reaction almost completely takes place next to the counter electrode. This can be seen in the large average reaction rate density. With the time the reaction spreads deeper into the electrode and at $t = 6000$ s

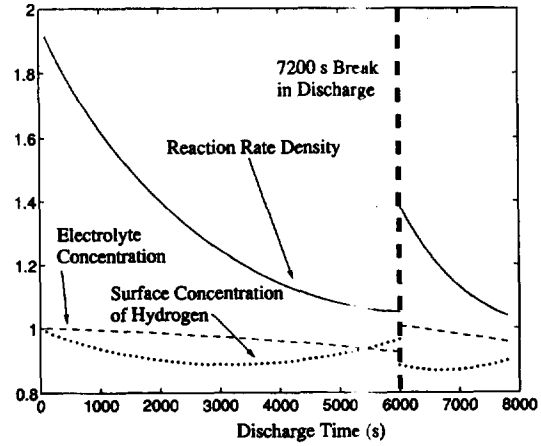

Fig. 7. Relative values of averaged reaction rate density, $\bar{r}/r_0$, electrolyte concentration, $\bar{c}/c_0$, and surface concentration of hydrogen, $\bar{h}_s/h_\infty$. The curves before and after the break are separated with a dashed line.

the reaction rate density is almost uniform as indicated by the value of about 1 of the relative average reaction rate density. During the discharge, the electrolyte concentration decreases away from the counter electrode. Thus, as the reaction moves further into the electrode it experiences lower electrolyte concentration as seen in Fig. 7. In the relative average hydrogen concentration, we see the effect of the decreasing total supply of hydrogen causing the increase observed before the break.

From Figs. 3, 6, and 7 and Eq. (44) it is easy to see that the reaction rate density dominates the behavior of the reaction overpotential. Before the break, the reaction takes place in the middle of the MH electrode and is almost completely spread out. At the restart of the discharge the reaction is again relatively localized next to the counter electrode and an increase in reaction overpotential is developed. The increase in electrolyte concentration and the decrease in surface concentration of hydrogen have a decreasing and an increasing effect on the reaction overpotential, respectively.

In the concentration polarization loss there are two competing factors and the change is small. It appears that here the increase in electrolyte concentration overrides the effect of the decreasing surface concentration of hydrogen. As a result, a 3 mV decrease in the concentration polarization loss is produced.

4.3. Hydrogen concentration during a break

We now study closer the most important factor in the electrode recovery, the hydrogen concentration change during a discharge break. The leveling of the hydrogen shown in Fig. 4 allows the reaction to start again from the counter electrode, which leads to the decrease in total potential loss.

Let t_c be the time when the discharge is interrupted. The corresponding level steady-state hydrogen concentration $h_\infty(t_c)$ is defined by Eq. (41). That is, $h_\infty(t_c)$ is the concentration towards which the hydrogen concentration in the electrode converges after the discharge has been interrupted at time t_c.

To estimate roughly the rate of convergence of the hydrogen we assume that the diffusion and the migration in the electrolyte are infinitely fast and there is no electric resistance in the solid. We also assume that the hydrogen diffusion in the MH particles is infinitively fast and that the electrolyte concentration and the potential difference between the solid and the electrolyte take their steady-state values c_0 and $V_{0,\infty}$ immediately after the current has been switched off. We also assume that the hydrogen diffusion in the MH particles is infinitely fast. With these assumptions the surface concentration of hydrogen satisfies for $t \geq t_c$

$$\frac{\partial}{\partial t}h_s(t,x) = -\frac{\rho}{F}\left[k_a \exp\left\{\frac{0.5FV_{0,\infty}(t_c)}{RT}\right\}c_0 h_s(t,x) - k_c \exp\left\{\frac{-0.5FV_{0,\infty}(t_c)}{RT}\right\}c_{H_2O}\right] \quad (46)$$

where

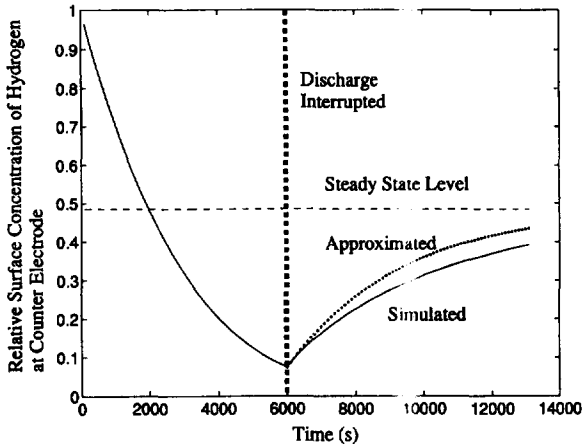

Fig. 8. Comparison between the simulated and the approximated surface concentration of hydrogen (Eq. (48)) next to the counter electrode at $x = x_1$ during the discharge break. The dashed vertical line marks the time when the discharge was interrupted and the dashed horizontal line corresponds the hydrogen concentration with the remaining hydrogen at $t = 6000$ s evenly distributed in the electrode.

$$V_{0,\infty}(t_c) = \frac{RT}{F}\ln\left\{\frac{k_c c_{H_2O}}{k_a c_0 h_\infty(t_c)}\right\} \quad (47)$$

It is easy to see that the solution is

$$h_s(t,x) = h_\infty(t_c) + (h_s(t_c,x) - h_\infty(t_c))\exp\left\{-\frac{t-t_c}{\tau(t_c)}\right\} \quad (48)$$

where the characteristic time, τ, is given by

$$\tau(t_c) = \frac{F}{\rho k_a c_0}\exp\left\{-\frac{0.5FV_{0,\infty}(t_c)}{RT}\right\} \quad (49)$$

Hence the hydrogen concentration converges exponentially towards the steady state h_∞.

Substituting the values for the parameters we find that if $t_c = 6000$ s corresponding to the state of discharge of about 50% then $\tau \approx 3500$ s, which fits the results reasonably well. A comparison of the approximation and the simulated surface concentration of hydrogen is presented in Fig. 8, in which the situation right next to the counter electrode is investigated. We notice that the characteristic time given above appears to be too short, that is, the concentration given by Eq. (48) converges too rapidly.

The main reason for this is that after the current has been cut there still exist non zero electrolyte concentration and potential gradients that sustain the ion flux of the leveling process. As a result the electrolyte concentration and potential differ from their level steady-state values. Taking this into account in Eq. (46) and solving for the surface concentration of hydrogen corresponding to the balance condition

$$\frac{\partial}{\partial t}h_s(t,x) = 0 \quad (50)$$

we obtain

$$h_s(t,x) = \frac{k_c c_{H_2O}}{k_a c(t,x)}\exp\left\{-\frac{FV(t,x)}{RT}\right\} \quad (51)$$

This hydrogen concentration at a given time, t, deviates from h_∞ towards the concentration before the break and the deviation is naturally at its largest values immediately after the discharge has been interrupted. Consequently, the simulated convergence is slower than the approximated one. Moreover, the lower the porosity of the MH electrode the larger are the electrolyte concentration and potential gradients. Thus, lower porosity leads to slower convergence of hydrogen concentration.

Note that τ is a decreasing function of t and that $\tau(t_{max}) = 0$ s. This behavior is explained easily. The more the electrode is discharged the smaller amount of hydrogen has to move in the process of convergence to the constant steady state.

5. Conclusions

With the average losses, see Ref. [3], the average electrolyte and hydrogen concentration, and the average reaction rate density presented in this article it is easy describe and analyze the discharge performance of a thick MH electrode.

These tools were applied in studying a break of discharge. It is clear that the dominating factor in the recovery of the electrode during a break is the decreasing potential loss in the electrolyte.

The changes in the degree of localization of the reaction determine the behavior of the second most important source of loss, the reaction overpotential. In the middle of the discharge the reaction is almost completely uniform but in the beginning, and especially in the end of the discharge, the reaction is strongly localized causing an increase in reaction overpotential.

We developed a simple model for estimating the leveling of the hydrogen concentration during a break, which is the basic phenomenon in the recovery of a thick MH electrode.

6. List of symbols

c	electrolyte concentration, mol/m^3
$\bar{c}$	average electrolyte concentration, mol/m^3
c_0	initial concentration of the electrolyte, mol/m^3
c_{H_2O}	concentration of water in the electrolyte, mol/m^3
d	pseudo diffusion coefficient in the hydrogen diffusion model, m^2/s
D_{free}	integral diffusion coefficient of KOH, m^2/s
D^+	effective diffusion coefficient of K^+ ions, m^2/s
D^-	effective diffusion coefficient of OH^- ions, m^2/s
D^+_{free}	diffusion coefficient of K^+ ions, m^2/s
D^-_{free}	diffusion coefficient of OH^- ions, m^2/s
D^H	diffusion coefficient of hydrogen in the MH alloy, m^2/s
F	Faraday's constant, 96 500 C/mol
h	hydrogen concentration in MH alloy, mol/m^3
h_0	initial concentration of hydrogen in MH alloy, mol/m^3
h_∞	steady-state concentration of hydrogen, mol/m^3
h_s	surface concentration of hydrogen in the MH alloy, mol/m^3
$\bar{h}_s$	average surface concentration of hydrogen in the MH alloy, mol/m^3
J	discharge flux density, mol/m^{2}s
k_a	anodic reaction rate constant, m^6/(kg mol s)
k_c	cathodic reaction rate constant, m^3/(kg s)
L	total length of the cell, m
r	reaction rate density in the MH electrode, mol/(m^3 s)
$\bar{r}$	average reaction rate density in the MH electrode, mol/(m^3 s)
r_0	reference reaction rate density in the MH electrode, mol/(m^3 s)
r_{MH}	diffusion distance in real MH particles, m
R	universal gas constant, 8.3143 J/(mol K)
t	time, s
t^+	transference number of K^+ ions
t_c	time when the discharge is interrupted, s
t_{diff}	characteristic diffusion time in MH particles, s
t_{max}	maximal discharge time, s
T	temperature, K
V	potential difference between the MH electrode and the electrolyte vs. Hg/HgO, V
V_{loss}	total potential loss in the MH electrode, V
V_0	local momentary equilibrium potential vs. Hg/HgO, V
$V_{0,\infty}$	steady-state open-circuit equilibrium potential vs. Hg/HgO, V
x	spatial coordinate across the electrode, m
x_c	location of the current collector, m
x_l	location of the counter electrode and the left end of the MH electrode, m
x_r	location of the right end of the MH electrode, m
z	spatial coordinate in the hydrogen diffusion model, m
Z	maximum diffusion distance in the hydrogen diffusion model, m

Greek letters

γ	active surface area density in the MH electrode, 1/m
δ_ξ	Dirac's delta function located at $x = \xi$
ϵ	porosity of the MH electrode
Λ_{free}	equivalent conductance of KOH, S m^2/mol
η	reaction overpotential, V
η_l	potential loss in the electrolyte, V
η_p	concentration polarization loss, V
η_s	potential loss in the solid phase, V
$\bar{\eta}$	average reaction overpotential, V
$\bar{\eta}_l$	average potential loss in the electrolyte, V
$\bar{\eta}_p$	average concentration polarization loss, V
$\bar{\eta}_s$	average potential loss in the solid phase, V
κ	effective conductivity of the electrode material, S/m
ν	MH volume fraction

ϕ electric potential in the electrolyte, V
φ electric potential in the solid phase, V
Φ electrode potential vs. Hg/HgO, V
ρ density of the MH material, kg/m^3
σ^+ effective ionic conductivity of K^+ ions, S/m
σ^- effective ionic conductivity of OH^- ions, S/m
σ^+_{free} ionic conductivity of K^+ ions, S/m
σ^-_{free} ionic conductivity of OH^- ions, S/m
τ characteristic time of convergence of hydrogen to the steady state, s

References

[1] M. Viitanen, *J. Electrochem. Soc., 140* (1993) 936.
[2] P. De Vidts, J. Delgado and R.E. White, *J. Electrochem. Soc., 143* (1995) 3972–3981.
[3] J. Heikonen, K. Vuorilehto and T. Noponen, *J. Electrochem. Soc.*, to be published.
[4] Z. Mao, P. De Vidts, R.E. White and J. Newman, *J. Electrochem. Soc., 141* (1994) 54.
[5] T.F. Fuller, M. Doyle and J. Newman, *J. Electrochem. Soc., 141* (1994) 982.
[6] R. Pollard and J. Newman, *J. Eletrochem. Soc., 128* (1981) 503.
[7] J. Heikonen, T. Noponen and M. Lampinen, *J. Power Sources*, to be published.
[8] J.S. Newman, *Electrochemical Systems*, Prentice Hall, Englewood Cliffs, NJ, 2nd edn., 1991.
[9] V.M.M. Lobo and J.L. Quaresma, *Electrolyte Solutions: Literature Data on Thermodynamic and Transport Properties*, Vol. II, Coimbra Editore, Coimbra, Portugal, 1981.
[10] S.U. Falk and A.J. Salkind, *Alkaline Storage Batteries*, Wiley, New York, 1969.
[11] A. Züttel, F. Meli and L. Schlapbach, *J. Alloys Comp., 221* (1995) 207.